Modelling of a Spatially Correlated MIMO Wireless Channel

B.B. Varghese* and B.T. Maharaj**

** Dept. of Electrical, Electronic and Computer Eng. Univ. of Pretoria, Lynnwood Road, South Africa, 0002, e-mail: benubobben@yahoo.com*
*** Dept. of Electrical Electronic and Computer Engineering, Univ. of Pretoria, Lynnwood Road, South Africa, e-mail:sunil.maharaj@up.ac.za*

Abstract: The channel capacity of a wireless communication system is greatly increased with the usage of multiple antennas at both the transmitter and receiver as long as the environment provides sufficient scattering. This paper shows a new geometric MIMO channel model that has taken the path loss parameter into account, as well as non-isotropic scattering at both ends of the radio link. Separate transmit and receive correlation functions are derived in a compact closed format, which includes some key parameters, such as distance between transmitter and receiver, antenna element spacing and degree of scattering. The capacity of the MIMO fading channel with varying number of antenna elements, distance between transmitter and receiver, various environments, varying signal to noise ratio at the receiver, varying the antenna element spacing at the transmitter and the degree of scattering at transmitter and receiver are investigated and shown for this model.

Key words: correlation, fading channels, MIMO, non-isotropic scattering, path loss.

1. INTRODUCTION

Multiple Input Multiple Output (MIMO) systems employ multiple antennas at both transmitter and receiver and were firstly reported by Teletar, [1] and Foschini, Gans, [2] that can be dated back to 1995. It was shown that MIMO channels could offer larger gains in capacity than the traditional Single Input Single Output (SISO) channel using the Shannon Capacity formula.

The need for high data rate in wireless communications coupled with the problem of power and bandwidth restrictions, as well as the multipath fading channel has increased profusely in the recent years. Due to this, much attention has been given to research of antenna arrays in mobile and fixed wireless communication systems.

Many research papers have been presented on MIMO systems in areas as diverse as channel modeling, information theory and coding, signal processing, antenna design and multi- antenna cellular design for fixed and mobile wireless communications. This paper is an extended version of [3] that is based on MIMO channel modeling which investigates the effects of correlation and path loss on a multiple element antenna transmission and reception system. An overview of the different models for MIMO propagation is shown in [4]

Some of these models can be categorized into two different groups based on the location of the scatterers. The first group consists of scatterers present only at the User (receiver) as shown in [5], [6] and [7] while the second has scatterers situated at the Base station and the User [8].

The most common communication model is based on the first group where the base station is in an elevated position and lies unobstructed by local scatterers. The User is situated at ground level where there are a large number of local scatterers due to the different objects (like vegetation, landscape, buildings, etc) surrounding the User.

The second group is another communication model that has recently been given some attention. In this group, both the base station and user are considered to be surrounded by a large number of local scatterers. Even though the base station is elevated, it can also be obstructed by tall buildings, trees or hilly areas.

Much research has been done on the first group of models, by investigating the effects of correlation on a multiple element antenna transmission and reception system while only a few have been done on the second group model.

This paper presents a new geometric model for a fixed MIMO channel, which is almost similar to the second group where there is non-isotropic scattering at both the transmitter and receiver. This model has considered different parameters together that will affect the correlation in a MIMO channel. All the previous models have only investigated a few of these parameters and not all of them.

The different parameters considered are the inclusion of the path loss parameter, n, the distance between the transmitter and receiver and the scatterers present at both transmitter and receiver. We consider a circular ring of scatterers to surround the user as shown in [9], while a ring of scatterers surrounds the base station. Also path loss is considered, which depends upon the distance between the transmitter and receiver. It also depends upon the environment, which may be urban, rural, indoor

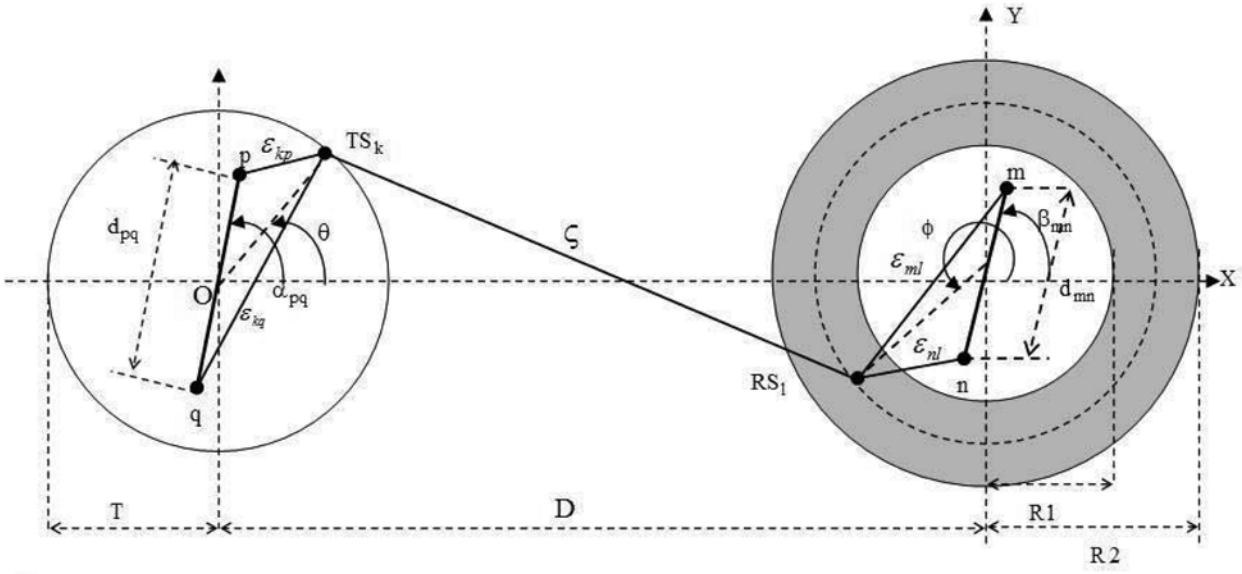

Figure 1: Geometric Model for a 2 x 2 MIMO channel

or outdoor [10]. Separate transmit and receive antenna correlation functions are derived from this model. Capacities for this model for different environments under different assumptions are presented.

This paper is organized as follows. The geometric MIMO channel model is shown and described in section 2 with its corresponding cross correlation functions that has been derived in section 3. The calculation of the capacity and the simulation results are presented in section 4 and finally in section 5, conclusions are drawn.

2. THE NEW MIMO CHANNEL MODEL

Consider a narrowband single user communication system with two transmit and two receive omni-directional antenna elements as shown in Fig 1. No line of sight (NLOS) is assumed. Since the user or receiver is subjected to more scatterers that may not necessary lie in a ring format, it is assumed that the scatterers can be located at any point on the circular ring. The distance of the scatterers on the circular ring to the user ranges between R1 and R2. Both the transmitter and receiver are assumed to be fixed and the distance between them is D with α_{pq} and β_{mn} as the angles the antenna arrays form with the horizontal axis. The input / output relation of this MIMO system can be written as

$$\bar{y}(t) = H(t)\bar{x}(t) + \bar{n}(t) \qquad (1)$$

Where: $\bar{x}(t)$ is the transmit vector that contains elements $x_j(t)$, which denotes the signal transmitted from antenna $j = \{1,...,n_T\}$, where n_T is the number of transmitter antenna elements and in this case $n_T = 2$.

$\bar{y}(t)$ is the receive vector that contains elements $y_i(t)$, which denotes the signals received by antenna $i = \{1,...,n_R\}$, where n_R is the number of receiver antenna elements and in this case $n_R = 2$.

$\bar{n}(t)$ is the noise vector that contains elements $n_i(t)$, which denotes the additive white Gaussian noise (AWGN) at the receiver antenna.

$H(t)$ is a $n_R \times n_T$ channel matrix of complex path gains $H_{ij}(t)$ between transmit antenna j and receive antenna i.

Certain assumptions are made for Fig.1, which are similar to [7]-[9]. It is assumed that K scatterers lie on the ring of radius T at the base station where the k^{th} transmit scatterer is denoted by TS_k. Similarly L scatterers lie on the circular ring of radius $R1 \le R \le R2$ where the 1^{th} scatterer is denoted by RS_l. Each scatterer introduces a gain and phase shift and is assumed to be dependent on the direction of the ray's arrival. The gain and phase shift introduced by RS_l from a ray received from TS_k is different from that introduced by another ray received from another scatterer, say TS_k'.

It is also assumed that rays from different antenna elements arrive at a scatterer at the same angle and so for a particular scatterer, the gain and phase shift is the same for rays coming from different antenna elements. The joint gain and phase shift of TS_k and RS_l is denoted by g_{lk} and ψ_{lk}.

Since K is the number of independent scatterers surrounding the base station and L is the number of independent scatterers surrounding the user, it can be assumed that as K and L tends to infinity.

$$\frac{1}{KL}\sum_{k=1}^{K}\left\{\sum_{l=1}^{L}E\left[g_{lk}^{2}\right]\right\}=1 \tag{2}$$

The channel gain h_{mp} for the link between base station antenna element p and user antenna element m is given by the equation:

$$h_{mp}(t)=\sqrt{\Omega_{mp}}\lim_{K,L\to\alpha}\frac{1}{\sqrt{KL}}\sum_{k=1}^{K}\sum_{l=1}^{L}g_{lk}(d)^{-n/2} \times\exp\left[j\psi_{lk}-\frac{j2\pi}{\lambda}\left(\varepsilon_{kp}+\varsigma+\varepsilon_{ml}\right)\right] \tag{3}$$

Here h_{mp} is a Rayleigh fading process obtained from the central limit theorem which implies that h_{mp} is a low pass, zero mean, complex Gaussian random process, similar to [11] and n is the path loss parameter depending upon the environment as shown in [10, page 139]. The power transferred through this link is Ω_{mp} and $\varepsilon_{kp}, \varsigma$ and ε_{ml} are the distances as shown in Fig.1. The distance, d traveled by the ray can be written as:

$$d=T+\varsigma+R \tag{4}$$

From the diagram, ς can be calculated under certain assumptions. Consider the triangle ΔOTS_kRS_l and assume $D >> R1, R2$, then the distance $ORS_l \approx (D-R)$ Applying the law of cosines:

$$\varsigma^2=T^2+(D-R)^2-2T(D-R)\cos\mu_T \tag{5}$$

Hence ς can be written as:

$$\varsigma=\sqrt{T^2+(D-R)^2-2T(D-R)\cos\mu_T} \tag{6}$$

Where $\mu_T\in(-\pi,\pi)$ is the mean angle at which the scatterers are distributed on the ring.

3. DERIVATION OF THE CROSS CORRELATION FUNCTION

A joint space-time cross correlation function is derived from the model shown in Fig.1 in a manner that is similar to [6]. The correlation between two links mp and nq for a time delay τ can be defined as:

$$\rho_{mp,nq}(t,\tau)=E\left[h_{mp}(t)h_{nq}^{*}(t+\tau)\right]/\sqrt{\Omega_{mp}.\Omega_{nq}} \tag{7}$$

Where Ω_{mp} is the power transferred from the transmitter antenna p to the receiver antenna m and Ω_{nq} is the power transferred from the transmitter antenna q to the receiver antenna n. Here * indicates the complex conjugate and

$$h_{nq}^{*}(t+\tau)=\sqrt{\Omega_{nq}}\lim_{K,L\to\alpha}\frac{1}{\sqrt{KL}}\sum_{k=1}^{K}\sum_{l=1}^{L}g_{lk}(d)^{-n/2} \times\exp\left[-j\psi_{lk}+\frac{j2\pi}{\lambda}\left(\varepsilon_{kq}+\varsigma+\varepsilon_{nl}\right)\right] \tag{8}$$

After substitutions, (7) gives:

$$\rho_{mp,nq}(t,\tau)=\lim_{K,L\to\alpha}\frac{1}{KL}\sum_{k=1}^{K}\left\{\sum_{l=1}^{L}E\left[g_{lk}^{2}\right](d)^{-n}\right\} \times\exp\left(\frac{-j2\pi}{\lambda}\left(\varepsilon_{kp}+\varepsilon_{ml}-\varepsilon_{kq}-\varepsilon_{nl}\right)\right) \tag{9}$$

Since the receiver is assumed to be fixed and the channel is in a quasi-static state, it can be written:

$$\rho_{mp,nq}(t,\tau)=\rho_{mp,nq}(\tau)=\rho_{mp,nq} \tag{10}$$

As K and L approach infinity, (3) can be written as [9], [12]:

$$\lim_{K,L\to\alpha}\frac{E\left|g_{lk}^{2}\right|}{KL}(d)^{-n} =(d)^{-n}p(\theta)p(\phi,R)d\theta d\phi dR \tag{11}$$

Where $p(\theta)$ and $p(\phi,R)$ are the probability distributions of both the transmit and receive scatterers. Substituting the above relation in (9):

$$\rho_{mp,nq}=(d)^{-n}\int_{R1}^{R2}\int_{-\pi}^{\pi}\int_{-\pi}^{\pi}\exp\left\{-\frac{j2\pi}{\lambda}\left(\varepsilon_{\theta p}+\varepsilon_{m\phi}-\varepsilon_{\theta q}-\varepsilon_{n\phi}\right)\right\} \times p(\theta)p(\phi,R)d\theta d\phi dR \tag{12}$$

$\varepsilon_{\theta p}$ is the distance from p to the ring of transmitter scatterers TS_k at an angle θ from the ring centre. All the other terms are defined in the same manner.

By using the law of cosines, (12) can be calculated numerically from the following equations:

$$\varepsilon_{\theta p}^2 = \frac{d_{pq}^2}{4} + T^2 - d_{pq} T \cos(\alpha_{pq} - \theta)$$

$$\varepsilon_{\theta q}^2 = \frac{d_{pq}^2}{4} + T^2 + d_{pq} T \cos(\alpha_{pq} - \theta)$$

$$\varepsilon_{m\phi}^2 = \frac{d_{mn}^2}{4} + R^2 - d_{mn} R \cos(\phi - \beta_{mn})$$

$$\varepsilon_{n\phi}^2 = \frac{d_{mn}^2}{4} + R^2 + d_{mn} R \cos(\phi - \beta_{mn}) \quad (13)$$

Where d_{pq} is the antenna element spacing at the transmitter and d_{mn} is the antenna element spacing at the receiver.

Assuming the following:

$T >> d_{pq}, R >> d_{mn}$, $\lim_{x \to 0} \sin x \approx x$ and

$\lim_{x \to 0} \sqrt{1+x} \approx 1 + \frac{x}{2}$,

the equations in (11) can be simplified to:

$$\varepsilon_{\theta p} \approx T - \frac{d_{pq}}{2} \cos(\alpha_{pq} - \theta)$$

$$\varepsilon_{\theta q} \approx T + \frac{d_{pq}}{2} \cos(\alpha_{pq} - \theta)$$

$$\varepsilon_{m\phi} \approx R - \frac{d_{mn}}{2} \cos(\phi - \beta_{mn})$$

$$\varepsilon_{n\phi} \approx R + \frac{d_{mn}}{2} \cos(\phi - \beta_{mn}) \quad (14)$$

Assuming $p(\phi, R) = p(\phi)p(R)$, the scatterer distribution used here for the transmitter, $p(\theta)$ and the receiver, $p(\phi)$ is the von Mises PDF [13] which provides closed form solutions and is given by

$$p(\theta) = \frac{1}{2\pi . I_0(\kappa_T)} \exp[\kappa_T \cos(\theta - \mu_T)]$$

$$p(\phi) = \frac{1}{2\pi . I_0(\kappa_R)} \exp[\kappa_R \cos(\phi - \mu_R)] \quad (15)$$

where $\theta, \phi \in (-\pi, \pi)$, κ_T and κ_R are the scattering parameters at the transmitter and receiver, μ_T and μ_R are the mean angles at which the scatterers are assumed to be distributed on the ring and $I_0(.)$ is the zero order modified Bessel function.

By splitting the terms in (12) into two different groups, one containing θ that represents the transmitter (TX) correlation, $\rho_{p,q}^{TX}$ and the other containing ϕ that represents the receiver (RX) correlation, $\rho_{m,n}^{RX}$, the joint antenna correlation can be written as [6], [7] & [8]:

$$\rho_{mp,nq} \approx \rho_{pq}^{TX} . \rho_{mn}^{RX} \quad (16)$$

Taking the attenuation factor, n in the TX side, the separate transmit and receive antenna correlation is written as

$$\rho_{pq}^{TX} = (d)^{-n} \int_{-\pi}^{\pi} \exp\left\{-\frac{j2\pi}{\lambda}\left(\varepsilon_{\theta p} - \varepsilon_{\theta q}\right)\right\} p(\theta) d\theta$$

$$\rho_{mn}^{RX} = \int_{R1}^{R2} \int_{-\pi}^{\pi} \exp\left\{-\frac{j2\pi}{\lambda}\left(\varepsilon_{m\phi} - \varepsilon_{n\phi}\right)\right\} p(\phi) p(R) d\phi dR \quad (17)$$

Substituting (14) in (17):

$$\rho_{pq}^{TX} = (d)^{-n} \int_{-\pi}^{\pi} \exp\left\{-\frac{j2\pi}{\lambda}\left(-d_{pq} \cos(\alpha_{pq} - \theta)\right)\right\} p(\theta) d\theta$$

$$\rho_{mn}^{RX} = \int_{R1}^{R2} \int_{-\pi}^{\pi} \exp\left\{-\frac{j2\pi}{\lambda}\left(-d_{mn} \cos(\phi - \beta_{mn})\right)\right\} p(\phi) p(R) d\phi dR \quad (18)$$

After further simplifications:

$$\rho_{pq}^{TX} = (d)^{-n} \int_{-\pi}^{\pi} \exp\left\{\frac{j2\pi}{\lambda} d_{pq} \cos(\alpha_{pq} - \theta)\right\} p(\theta) d\theta$$

$$\rho_{mn}^{RX} = \int_{R1}^{R2} \int_{-\pi}^{\pi} \exp\left\{\frac{j2\pi}{\lambda} d_{mn} \cos(\phi - \beta_{mn})\right\} p(\phi) p(R) d\phi dR \quad (19)$$

Substituting (15) in (19):

$$\rho_{pq}^{TX} = \frac{(d)^{-n}}{2\pi I_0(\kappa_T)} \int_{-\pi}^{\pi} \exp\left\{\frac{j2\pi}{\lambda} d_{pq} \cos(\alpha_{pq} - \theta)\right\} \times \exp\{\kappa_T \cos(\theta - \mu_T)\} d\theta$$

$$\rho_{mn}^{RX} = \frac{1}{2\pi I_0(\kappa_R)} \int_{R1}^{R2} \int_{-\pi}^{\pi} \exp\left\{\frac{j2\pi}{\lambda} d_{mn} \cos(\phi - \beta_{mn})\right\} \times \exp\{\kappa_R \cos(\phi - \mu_R)\} p(R) d\phi dR \quad (20)$$

Using the formula:

cos (A-B) = cosA.cosB + sinA.sinB, the equation (20) can be written as:

$$\rho_{pq}^{TX} = \frac{(d)^{-n}}{2\pi I_0(\kappa_T)} \times \int_{-\pi}^{\pi} \exp\left\{\begin{array}{l} \frac{j2\pi}{\lambda} d_{pq} \left[\cos\alpha_{pq} . \cos\theta + \sin\alpha_{pq} . \sin\theta\right] \\ + \kappa_T \left[\cos\theta . \cos\mu_T + \sin\theta \sin\mu_T\right] \end{array}\right\} d\theta$$

$$\rho_{mn}^{RX} = \frac{1}{2\pi I_0(\kappa_R)} \int_{R1}^{R2} \times \int_{-\pi}^{\pi} \exp\left\{ \begin{array}{l} \frac{j2\pi}{\lambda} d_{mn} [\cos\phi.\cos\beta_{mn} + \sin\phi.\sin\beta_{mn}] \\ + \kappa_R [\cos\phi.\cos\mu_R + \sin\phi.\sin\mu_R] \end{array} \right\} p(R) d\phi dR \quad (21)$$

Further simplifications give:

$$\rho_{pq}^{TX} = \frac{(d)^{-n}}{2\pi I_0(\kappa_T)} \times \int_{-\pi}^{\pi} \exp\left\{ \begin{array}{l} \cos\theta \left[\frac{j2\pi}{\lambda} d_{pq} \cos\alpha_{pq} + \kappa_T \cos\mu_T \right] \\ + \sin\theta \left[\frac{j2\pi}{\lambda} d_{pq} \sin\alpha_{pq} + \kappa_T \sin\mu_T \right] \end{array} \right\} d\theta$$

$$\rho_{mn}^{RX} = \frac{1}{2\pi I_0(\kappa_R)} \int_{R1}^{R2} \times \int_{-\pi}^{\pi} \exp\left\{ \begin{array}{l} \cos\phi \left[\frac{j2\pi}{\lambda} d_{mn} \cos\beta_{mn} + \kappa_R \cos\mu_R \right] \\ + \sin\phi \left[\frac{j2\pi}{\lambda} d_{mn} \sin\beta_{mn} + \kappa_R \sin\mu_R \right] \end{array} \right\} p(R) d\phi dR \quad (22)$$

Making use of the integration rule in [14] (page 336, equation 3.338-4):

$$\int_{-\pi}^{\pi} \exp(y \sin x + z \cos x) dx = 2\pi I_0(\gamma) \quad (23)$$

where $\gamma = \sqrt{y^2 + z^2}$ and the trigonometric rule $\cos^2 A + \sin^2 A = 1$, then (22) can be written as:

$$\rho_{pq}^{TX} = \frac{(d)^{-n}}{I_0(\kappa_T)} \times I_0 \left[\left(\kappa_T^2 + \left(\frac{j2\pi}{\lambda} d_{pq} \right)^2 + j \frac{4\pi}{\lambda} d_{pq} \kappa_T \cos(\mu_{TX} - \alpha_{pq}) \right)^{\frac{1}{2}} \right]$$

$$\rho_{mn}^{RX} = \frac{1}{I_0(\kappa_R)} \times I_0 \left[\left(\kappa_R^2 + \left(\frac{j2\pi}{\lambda} d_{mn} \right)^2 + j \frac{4\pi}{\lambda} d_{mn} \kappa_R \cos(\mu_{RX} - \beta_{mn}) \right)^{\frac{1}{2}} \right] \times \frac{2}{\left(R_2^2 - R_1^2 \right)} \int_{R1}^{R2} R dR \quad (24)$$

After further simplification, the TX correlation is given by:

$$\rho_{pq}^{TX} = \frac{(d)^{-n}}{I_0(\kappa_T)} I_0 \left[\left(\kappa_T^2 - c_{pq}^2 + j2c_{pq}\kappa_T \cos(\mu_{TX} - \alpha_{pq}) \right)^{\frac{1}{2}} \right] \quad (25)$$

Where $c_{pq} = \frac{2\pi d_{pq}}{\lambda}$ and κ_T is the scattering parameter at the transmitter.

Assuming $p(R) = 2R / \left(R_2^2 - R_1^2 \right)$ taken from [9], the RX correlation is given by

$$\rho_{mn}^{RX} = \frac{1}{I_0(\kappa_R)} I_0 \left[\left(\kappa_R^2 - b_{mn}^2 + j2b_{mn}\kappa_R \cos(\mu_{RX} - \beta_{mn}) \right)^{\frac{1}{2}} \right] \times \frac{2}{\left(R_2^2 - R_1^2 \right)} \int_{R1}^{R2} R dR \quad (26)$$

Where $b_{mn} = \frac{2\pi d_{mn}}{\lambda}$ and κ_R is the scattering parameter at the receiver.

By using the above closed form expressions in (25) and (26), one is able to determine some of the model characteristics as shown in the next section.

4. MODEL RESULTS

Let $\overline{U}$ be a $n_R \times n_T$ matrix of random, independent and zero mean complex Gaussian variates with unit variance and $\overline{X}$ be the $n_T \times n_T$ matrix of the transmit antenna correlation with matrix elements calculated from (25). Then the desired transmit antenna correlation is calculated by $x = \overline{U}\sqrt{\overline{X}}$. The channel matrix $\overline{H}$, between the transmitter and receiver can be calculated by $\overline{H} = x\sqrt{\overline{Y}}$, where $\overline{Y}$ is the $n_R \times n_R$ matrix of the receive antenna correlation with matrix elements calculated from (26).

From [1] and [2], the normalized channel Capacity for a particular realization H is given by

$$C = \log_2 \det \left[I_{n_R} + \frac{SNR}{n_T} \overline{HH}^H \right] \text{ b/s/Hz} \quad (27)$$

Where I_{n_R} is the $n_R \times n_R$ identity matrix, SNR is the average signal to noise ratio at the receiver, $\overline{H}^H$ is the conjugate transpose of $\overline{H}$ and $\det[.]$ is the determinant.

Simulations were done for this model for the following

general parameters SNR = 20dB, transmit carrier frequency = 2.4GHz (so $\lambda = 0.125$m), $\alpha_{pq} = \pi/2, \beta_{mn} = \pi/4$, $\kappa_R = 50$, R1=1m, R2=2m, T=1m, $\mu_{TX} = 0$, $\mu_{RX} = \pi$ and the antenna spacing for transmitter and receiver are $d_{mn} = d_{pq} = 0.3\lambda$.

The simulation in fig. 2 is the complementary cumulative distribution function (ccdf) versus capacity for various number of transmit and receive antenna elements. Here $\kappa_T = 10$, D =10m and n = 2.

Observing the figure, one can see that the capacity increases as the number of antennas increases. This graph shows the effect of scattering and the number of antenna elements present at both the transmitter and receiver. As the number of antenna elements goes on increasing, the capacity increase intervals gradually decreases.

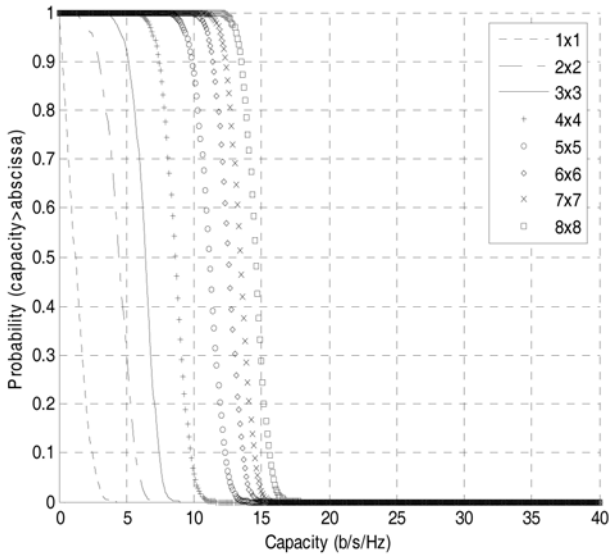

Figure 2. ccdf vs. capacity for varying antenna elements, $n_R x n_T$

The distance, D between the transmitter and receiver is varied as shown in fig 3. Here $\kappa_T = 10$ $\kappa_R = 50$ n=2 and $n_T = n_R = 8$.

It can be observed that as the distance between the transmitter and receiver increases, the capacity decreases. From the figure, one can see that the capacity varies most significantly when the distance between transmitter and receiver ranges from 5m to 10 m that is 5m < D < 10m and it gradually decreases in variation when the distance between transmitter and receiver is greater than 10m that is D > 10m at regular intervals of 5m.

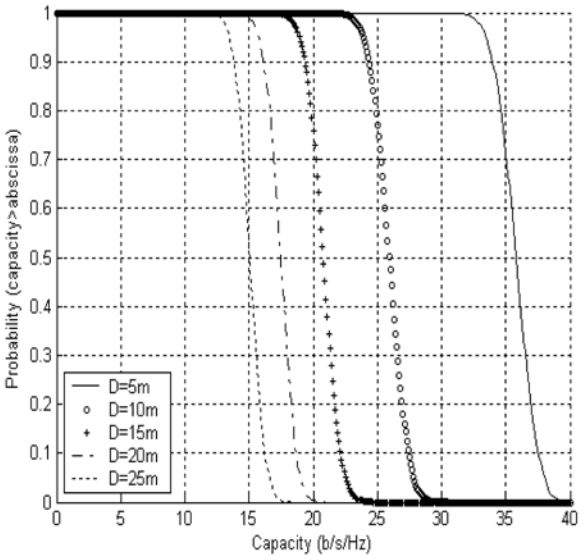

Figure 3. ccdf vs. capacity for varying distance between transmitter and receiver.

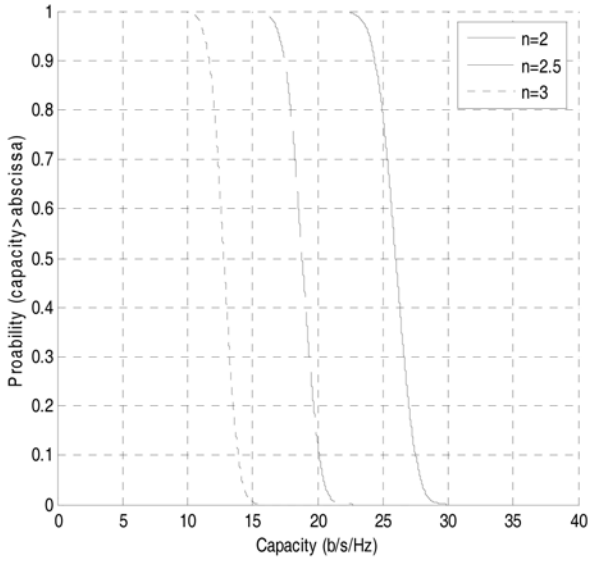

Figure 4. ccdf vs. capacity for varying path loss exponent (n).

For $\kappa_T = 10$, D=10 and $n_T = n_R = 8$, figure 4 shows the effect of the variation in the path loss exponent n, which depends on the environment used [10, page139]. For n=2 represents free space and for n between 2 to 6 represents either an urban area or an indoor no line of sight (NLOS). For n=1.6 represents an indoor line of sight (LOS) and the capacity will obviously be higher for the plotted values of n. This is not shown as this channel model is for a Rayleigh case.

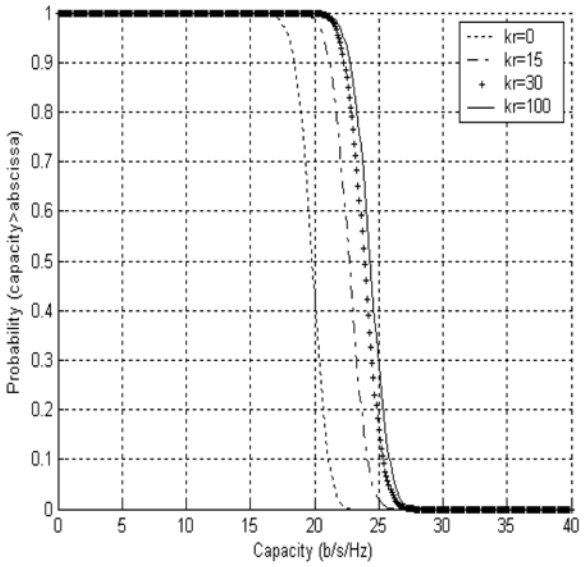

Figure 5. ccdf vs. capacity for varying scattering parameter at receiver.

Figure 5 shows the effect of the variation in the receiver scattering parameter κ_R. Here $\kappa_T = 5$, D=10m, $n_T = n_R = 8$ and n=2. For a 90% probability, the capacity increases by 4.5b/s/Hz for a κ_R increase from 0 to 30 and by only 0.5b/s/Hz for a κ_R increase from 30 to 100. This shows that the degree of scattering plays an important role in the enhancement of capacity for a MIMO system up to a certain point, where upon any further richness in scatterers has negligible effect on the capacity.

It was also found that if one varies the scattering parameter at the transmitter, κ_T, the capacity also increases for the same outage probability.

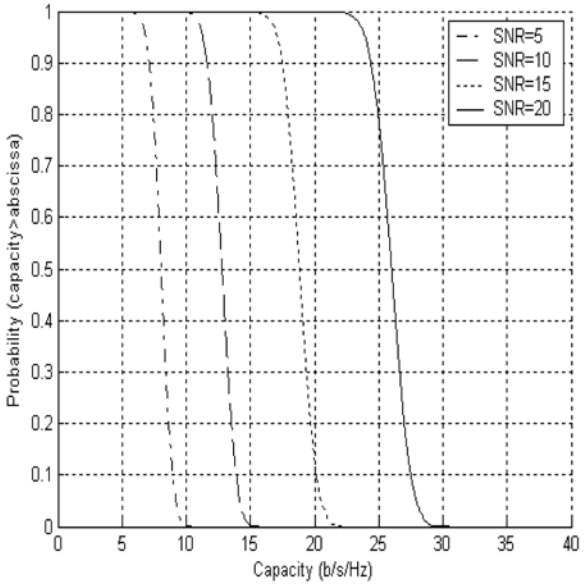

Figure 6. ccdf vs. capacity for varying signal to noise ratio (SNR) parameter.

In Figure 6, the effect of the variation of the signal to noise ratio (SNR) is shown, which is one of the most common and important parameter in a communication system. Here, $\kappa_T = 10$, $\kappa_R = 50$, D=10m, $n_T = n_R = 8$ and n=2. From the figure we can see as the signal to noise ratio increases, the capacity also increases as expected thus also validating the model. For a signal to noise ratio increase from 5dB to 10dB, the capacity increases by 5b/s/Hz for a 90% probability and from 10dB to 15dB, the capacity increases by 6b/s/Hz. The 15dB to 20dB signal to noise ratio increase shows a capacity increase of 7b/s/Hz for the same probability. This shows the effect of the signal to noise ratio on this channel model.

The effect of variation of the antenna element spacing at the transmitter is shown in fig 7. The SNR=20 dB, $\kappa_T = 10$, $\kappa_R = 50$, D=10m, $n_T = n_R = 8$, n=2 and $d_{mn} = 0.3\lambda$ was used in the computation. From the figure, one can see that as the antenna element spacing increases, the capacity automatically decreases to a certain extent. One observes that when $d_{pq} < 0.5\lambda$ and $d_{pq} > 0.8\lambda$, the capacity varies significantly. It was also found that when $d_{pq} > 1\lambda$, the capacity decreases very slightly, thus making it almost negligible.

It was also found that if one simultaneously varied the antenna spacing at the receiver, d_{mn}, the capacity decreases significantly for the same outage probability.

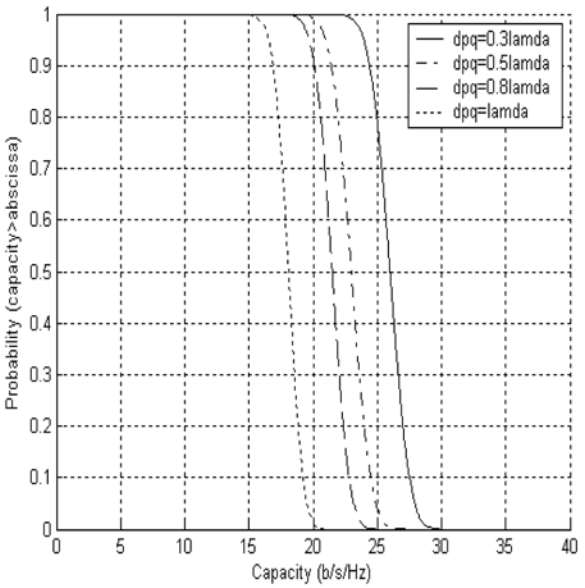

Figure 7. ccdf vs. capacity for varying antenna element spacing at the transmitter.

5. CONCLUSION

This model was developed for a fixed wireless indoor environment. A joint cross correlation function as well as separate transmit and receive correlation functions are derived. The effects of the number of antenna elements, the distance between the transmitter and receiver, the path loss exponent (environment), the signal to noise ratio (SNR), the degree of scattering at the receiver and the antenna element spacing at the transmitter are investigated and shown in the respective simulation graphs. From the results shown, it can be analyzed that the number of antenna elements, the signal to noise ratio and the distance between TX and RX has the most significant effect on the capacity.

This channel model was developed for separate transmit and receive correlation functions (Kronecker method). Further studies can be done by deriving a closed form joint correlation function for the same channel model by taking the same path loss exponent into account as well as the scattering at both ends of the radio link. Simulations can be plotted for the effect on capacity by varying the same parameters shown in this paper. They can then be compared with measured values [17] to show the more accurate method.

6. REFERENCES

[1] I. E. Telatar, "Capacity of multi-antenna Gaussian Channels," Tech. Rep. #BL0112170-950615-07TM, AT&T Bell Laboratories, 1995.

[2] G. J. Foschini and M. J. Gans, "On limits of wireless communication in a fading environment when using multiple antennas," *Wireless Personal Communications*, vol. 6, no. 3, pp.311-335, Kluwer Academic Publishers, March, 1998.

[3] B. B. Varghese and B. T. Maharaj, "A Spatially Correlated Model for MIMO Fading Channels," *Presented at the 12th ICT Wireless Comms and Technologies*, March 2005.

[4] K. Yu and B. Ottersten, "Models for MIMO propagation channels: a review," *Wiley Journal Wireless Communications and Mobile Computing*, vol.2, issues 7, pp.653-666, 2002.

[5] D. Shiu, G. J. Foschini, M. J. Gans and J. M. Kahn, "Fading correlation and its effect on the capacity of multielement antenna systems,"*IEEE Transactions on Communications*, vol.48, no.3, pp.502-513, 2000.

[6] Ali Abdi, Mostafa Kaveh, "A Space-Time Correlation Model for Multielement Antenna Systems in Mobile Fading Channels," *IEEE J. on Selected Areas in Comms.*, vol.20, no.3, pp.550-560, April, 2002.

[7] B.T.Maharaj and L.P.Linde, "Capacity for Spatial-Temporal Correlated MIMO Fading Channel," *Proceedings of IEEE AFRICON*, vol 1, pp.269-274, September, 2004.

[8] G. J. Byers and F. Takawira, "The Influence of Spatial and Temporal Correlation on the Capacity of MIMO Channels," *in Proc.IEEE WCNC 2003*, vol.1, pp. 359-364, March, 2003.

[9] Latinovic. Z.; Abdi. A.; Bar-Ness. Y, "A Wideband Space-Time Model for MIMO Mobile Fading Channels," *Wireless Communications and Networking, IEEE*, Vol.1, pp.338-342, March, 2003.

[10] T. S. Rappaport, " Path loss exponents for different environments*," in Wireless Communications: principles and practice*, 2nd edition, Upper Saddle River, N. J: Prentice Hall PTR, 2002.

[11] J. Fuhl, A. F. Molisch and E. Bonek, "Unified channel model for mobile radio systems with smart antennas," *IEEE Proc. Radar, Sonar and Navigation*, vol.145, pp.32-41, February, 1998.

[12] W. C. Jakes Jr., "Multipath interference," *in Microwave Mobile Communications*, W. C. Jakes Jr., Ed. New York: Wiley, 1974.

[13] A. Abdi, J. A. Barger and M. Kaveh, "A parametric model for the distribution of the angle of arrival and the associated correlation function and power spectrum at the mobile station," *IEEE Trans. Veh. Technol.*, vol.51, pp.425-434, May, 2002.

[14] I. S. Gradshteyn and I. M. Ryzhik, M. Young, *Table of Integrals, Series, and Products*. 6 th Edition, A. Jeffery, Editor, San Diego, CA: Academic Press, ISBN 0 – 12 – 294757 – 6, 2000.

[15] B. Holter, "On the Capacity of the MIMO channel-A tutorial Introduction," *in Proc. Norwegian Signal Processing Conference*, Trodheim, Norway, October, 2001.

[16] Lee, W. C. Y., *Mobile Communications Engineering*, McGraw Hill Publications, New York, 1985.

[17] B.T. Maharaj, J.W. Wallace, L.P. Linde and M.A. Jensen, "A low cost open-hardware wideband MIMO wireless channel sounder", *IEEE Transactions on Instrumentation and Measurement*, vol. 57, no. 10 , pp. 2283-2289, October 2008.

Bobby. B. Varghese received his B.Eng degree in Electronics and Communication in 2001 from Kuvempu University, Karnataka, India. He has also received his B.Sc. Hons degree in Applied Science in 2003 from University of Pretoria, Pretoria, South Africa. He is currently working as a Voice Engineer at Saab Grintek Technologies (Pty) Ltd, South Africa and also worked part time towards his MSc degree in Applied Science at the University of Pretoria.
His current fields of interests are Wireless Communications, MIMO systems, Mobile technologies including UMTS and HSDPA and VoIP.

B.T. Maharaj (SMSAIEE, M MIET) received both his BSc Eng. and MSc Eng. in Electronic Engineering from University of Natal. He also holds a MSc in Operational Telecommunications (Merit) (1996) from University of Coventry, UK and a PhD from University of Pretoria.
He worked for Electromagnetic Laboratory (EMLAB) Pty Ltd and Grinaker Avitronics Ltd. as a microwave design engineer. He subsequently worked at the Eastern Cape Technikon and is currently a working in the Department of Electrical, Electronic and Computer Engineering, University of Pretoria, South Africa. His research interests are in MIMO wireless systems, channel modeling and as well as Cognitive Radio.